IEEE Access
Multidisciplinary | Rapid Review | Open Access Journal

Received June 26, 2018, accepted July 23, 2018, date of publication August 1, 2018, date of current version August 28, 2018.

Digital Object Identifier 10.1109/ACCESS.2018.2862163

Adaptive Fuzzy Output Feedback Control of a Nonholonomic Wheeled Mobile Robot

SHUYING PENG AND WUXI SHI
Tianjin Polytechnic University, Tianjin 300387, China
Tianjin Key Laboratory of Advanced Technology of Electrical Engineering and Energy, Tianjin 300387, China
Corresponding author: Wuxi Shi (shiwuxi@163.com)

This work was supported in part by the Program for Innovative Research Team in the University of Tianjin, under Grant TD13-5036, and in part by the Natural Science Foundation of Tianjin, China, under Grant 15JCYBJC47800.

ABSTRACT This paper addresses the output feedback trajectory tracking problem for a nonholonomic wheeled mobile robot in the presence of parameter uncertainties, external disturbances, and a lack of velocity measurements. An unknown function is approximated by the fuzzy logic system, and an adaptive fuzzy observer is introduced. Then, by combining the kinematic model with the dynamic model, a control strategy is proposed that integrates an auxiliary velocity controller with an integral terminal sliding mode controller. By applying the proposed control strategy, it is proven that all of the signals in the closed system are bounded and that the auxiliary velocity tracking errors converge to a neighborhood of the origin in finite time. Therefore, the tracking position errors converge asymptotically to a small neighborhood near the origin with a faster response than achieved by other existing controllers. The simulation results demonstrate the effectiveness of the proposed strategy.

INDEX TERMS Wheeled mobile robot, adaptive fuzzy control, output feedback control, finite time convergence.

I. INTRODUCTION

A wheeled mobile robot (WMR) is an uncertain non-linear multiple-input multiple-output dynamic system. When the WMR constrains the wheel's ''pure rolling without slipping'' motion, it is also a typical kind of nonholonomic system that can be characterized by kinematic constraints. As a result, Brockett's necessary condition for asymptotic stabilization cannot be satisfied. Although there are so many characteristics that are difficult to handle, there has been tremendous research on the trajectory tracking problem of a nonholonomic WMR (NWMR) over the past several decades.

With the assumption of ''perfect velocity tracking'', a kinematic controller for the NWMR was designed in [1]. However, the dynamic model of the NWMR has been neglected, and it is not easy to realize perfect velocity tracking. Based on the backstepping technique, Fierro and Lewis [2] presented a dynamical extension that combines a kinematic controller with a torque controller. However, it was assumed that both the dynamic structure and the parameters of the NWMR are completely known. Considering the parameter uncertainties and external disturbances in practical WMRs, researchers have used a variety of non-linear control techniques, such as adaptive control [3], [4], robust adaptive control [5], [6], fuzzy logic control [7], neural network control [8], and sliding mode control [9]. It is noted that time-delayed control [10] is an alternate robust control method which does not depend on any uncertainty bounds. This method merges all the uncertain terms into a single lumped unknown function and then approximates it using control input and state information of the immediate past time instant. Based on time-delayed control, robust control, adaptive-robust control, and adaptive sliding mode control were developed in [11]–[13]. These dynamic controllers share a common idea of choosing the wheel torque as the control input. However, the wheel is driven by the actuator in reality [14]. Most existing torque controllers, in which the wheel actuator dynamics have been neglected, could degrade the tracking control performance. Therefore, it is more reasonable to use the actuator voltage as the control input. Thus, the wheel actuator dynamics were combined with the dynamics of the NWMR, and the actuator voltage was employed as the control input in [14]–[16]. It should be noted that these proposed controllers are all based on full-state feedback and require the velocities of the NWMR, which are measured by devices such as tachometers. However, in practice, such devices are costly or are frequently corrupted by a

considerable amount of noise. This will increase the cost, volume, and weight of the system.

To deal with this problem, in [17], a highly filtered version of the auxiliary velocity tracking errors was adopted to avoid having the velocity measurements of the NWMR include parameter uncertainties and external disturbances. Roy *et al.* [18] proposed a position-only time-delayed controller, which uses only position information of present and past instances to estimate the velocity and acceleration terms. In fact, output feedback control, in which only position and orientation measurements are required, is also an appropriate method for avoiding velocity measurements of the NWMR. However, nonholonomic constraints and the centripetal and Coriolis matrix lead to quadratic terms of unmeasured velocities. This causes many of solutions proposed for the control robot manipulators (see [19] and the references therein) to be not directly applicable to the NWMR. To overcome this difficulty, by means of transformation matrices, adaptive observers [20], [21] and an interlaced observer [22] were developed to estimate the unmeasured velocities for the NWMR in the presence of parametric uncertainties. In addition, a new input-output model of the NWMR was developed by defining a suitable set of output equations [23]. Thereafter, a linear observer [24] was adopted to solve the trajectory tracking problem of the NWMR in the presence of parametric and non-parametric uncertainties by using a dynamic surface control approach. Similar to [23], a saturated output feedback controller was designed for the NWMR considering the actuator saturation problem and the absence of velocity sensors in practice simultaneously in [25]. High-gain observers were also applied to the trajectory tracking control of the NWMR in [26] and [27]. More results on the output feedback control are referred to [28] and [29]. It is noted that these dynamic controllers can all guarantee that the auxiliary velocity tracking errors converge to a neighborhood near the origin as the time goes to infinity. However, the finite-time convergence of the auxiliary velocity tracking errors cannot be guaranteed.

Terminal sliding mode control (TSMC), which was proposed in [30], is an effective scheme that can guarantee the finite-time convergence of the auxiliary velocity tracking errors. Additionally, similar to the linear sliding mode control, strong robustness with respect to uncertainties can be obtained by using the TSMC. However, the initial TSMC may cause a singularity problem around the equilibrium [31], which would result in an unbounded control signal. To avoid this problem, a non-singular terminal sliding mode control was developed in [32]–[34]. The continuous non-singular terminal sliding mode [32] was subsequently extended into a class of multiple-input multiple-output non-linear systems [35]. Furthermore, by utilizing integral operation, an integral terminal sliding mode control (ITSMC) was presented in [36] for a class of first-order systems. In addition to its strong robustness, finite-time convergence, and non-singularity, in the ITSMC design, the system can start on the integral terminal sliding mode surface at the initialization time. Therefore, the time required to reach the sliding mode surface is eliminated.

Based on the above discussion, in this paper, we design an adaptive fuzzy output feedback controller for the trajectory tracking problem of the NWMR. This NWMR has parameter uncertainties, external disturbances, and unmeasured velocity. In this method, a fuzzy logic system (FLS) is adopted to approximate the unknown function, and an adaptive fuzzy observer is developed to estimate the unmeasured velocities. The kinematic model and the dynamic model are considered together. An integral terminal sliding mode controller is proposed that utilizes the actuator voltage as the control input together with an auxiliary velocity controller. The main contribution of the proposed control strategy are as follows:

(1) the total uncertainties, unmeasured velocity, together with its quadratic terms, are taken into account and the resulted unknown function is approximated by the FLS;

(2) the integral terminal sliding mode controller can guarantee the finite-time convergence of the auxiliary velocity tracking errors.

Therefore, the tracking position errors converge asymptotically to a small neighborhood near the origin with a faster response than achieved by other existing controllers. In addition, all of the signals are bounded.

The remainder of this paper is organized as follows. Section 2 reviews some basics of the model of the NWMR, ITSMC and FLS. An adaptive fuzzy observer is introduced in Section 3. In Section 4, a control strategy is proposed that integrates an auxiliary velocity controller with an integral terminal sliding mode controller. Section 5 provides simulation results to highlight the performance of our method. Conclusions are given in Section 6.

II. PRELIMINARIES

In this section, we briefly review some basics of the NWMR model, ITSMC, and FLS.

A. MODEL OF THE NONHOLONOMIC WHEELED MOBILE ROBOT

We consider a typical example of the WMR, called Type (2,0) WMR in [37]. Such a WMR is composed of two driving wheels and one passive wheel. The two driving wheels are controlled independently by two actuators, which determine the motion and orientation, and the passive wheel prevents the robot from tipping over as it moves on a plane. Fig. 1 describes the posture of the WMR in Cartesian coordinates. Both driving wheels, each with the same radius r, are mounted on the same axis and are separated by $2R$. The centre of mass of the WMR is located at C. P is located in the midpoint of the two driving wheels of the WMR. The distance between P and C is d.

When the electrical part of the actuator is considered, the kinematic and dynamic equations of the NWMR can be written as follows, from [17]:

$$\dot{q} = S(q)\vartheta, \tag{1}$$

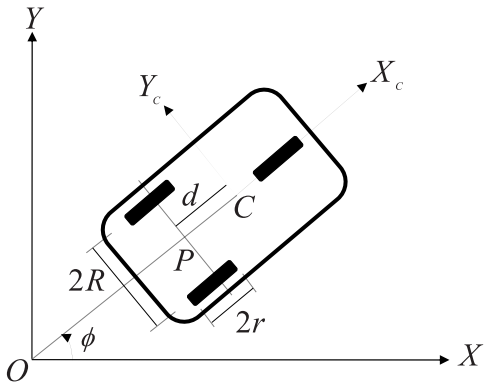

FIGURE 1. A wheeled mobile robot.

$$\overline{M}(q)\dot{\vartheta} + \overline{V}(q,\dot{q})\vartheta + \overline{F}(q,\dot{q}) + \overline{\tau}_d = \frac{NK_T}{R_a}\overline{B}u - \frac{N^2K_TK_b}{R_a}\overline{B}X\vartheta, \quad (2)$$

where

$$S(q) = \begin{bmatrix} \cos\phi & -d\sin\phi \\ \sin\phi & d\cos\phi \\ 0 & 1 \end{bmatrix},$$
$$\overline{M}(q) = \begin{bmatrix} m & 0 \\ 0 & I - md^2 \end{bmatrix},$$
$$\overline{V}(q,\dot{q}) = \begin{bmatrix} 0 & 0 \\ 0 & 0 \end{bmatrix},$$
$$\overline{B} = \frac{1}{r}\begin{bmatrix} 1 & 1 \\ R & -R \end{bmatrix},$$
$$X = \overline{B}^T.$$

$q = [x, y, \phi]^T$; $C(x, y)$ is the coordinate of C in the global coordinate frame XOY; and ϕ is the orientation of the local coordinate frame X_CCY_C attached to the WMR platform measured from the X axis and is called the heading angle of the WMR. $\vartheta = [\nu, \omega]^T$, where ν and ω are the linear velocity of point P along the robot axis and the angle velocity, respectively. $\overline{M}(q)$ is the inertia matrix, $\overline{V}(q,\dot{q})$ is the centripetal and Coriolis matrix, $\overline{F}(q,\dot{q}) = [\overline{F}_1, \overline{F}_2]^T$ is the surface friction, and $\overline{\tau}_d = [\overline{\tau}_{d1}, \overline{\tau}_{d2}]^T$ denotes bounded unknown disturbances, including unstructured unmodelled dynamics. N is the gear ratio, K_T is the motor torque constant, K_b is the counter electromotive force coefficient, and R_a is the electric resistance. $u = [u_1, u_2]^T$ is the actuator voltage input vector.

Remark 1: It is assumed that the NWMR has the parameter uncertainties $\bigtriangleup\overline{M}(q)$ of $\overline{M}(q)$ and $\bigtriangleup\overline{V}(q,\dot{q})$ of $\overline{V}(q,\dot{q})$. Then, the dynamic equation of the NWMR can be arranged in the following form:

$$\overline{M}(q)\dot{\vartheta} + \overline{V}(q,\dot{q})\vartheta + f = \frac{NK_T}{R_a}\overline{B}u - \frac{N^2K_TK_b}{R_a}\overline{B}X\vartheta, \quad (3)$$

where $f = [f_1, f_2]^T = \bigtriangleup\overline{M}(q)\dot{\vartheta} + \bigtriangleup\overline{V}(q,\dot{q})\vartheta + \overline{F}(q,\dot{q}) + \overline{\tau}_d$ represents the lumped uncertainties. It is noted that f is a function of $Y = [x, y, \phi, \nu, \omega]^T$. In this paper, we assume that $q = [x, y, \phi]^T$ is measurable but that $\vartheta = [\nu, \omega]^T$ is not. To design an observer to estimate ν and ω, we rewrite (1) and (3) as follows:

$$\begin{cases} \dot{x} = \nu\cos\phi - \omega d\sin\phi, \\ \dot{y} = \nu\sin\phi + \omega d\cos\phi, \\ \dot{\phi} = \omega, \\ \dot{\nu} = f_1(Y) + a_{11}U_1 - a_{12}\nu, \\ \dot{\omega} = f_2(Y) + a_{21}U_2 - a_{22}\omega. \end{cases} \quad (4)$$

where

$$U_1 = u_1 + u_2,$$
$$U_2 = u_1 - u_2,$$
$$a_{11} = \frac{NK_T}{R_a}\cdot\frac{1}{m}\cdot\frac{1}{r},$$
$$a_{12} = \frac{N^2K_TK_b}{R_a}\cdot\frac{2}{m}\cdot(\frac{1}{r})^2,$$
$$a_{21} = \frac{NK_T}{R_a}\cdot\frac{1}{I - md^2}\cdot\frac{R}{r},$$
$$a_{22} = \frac{N^2K_TK_b}{R_a}\cdot\frac{2}{I - md^2}\cdot(\frac{R}{r})^2.$$

Remark 2: Note that the quadratic terms of unmeasured velocities ν and ω are contained in the unknown functions $f_1(Y)$ and $f_2(Y)$ in the model of the NWMR (4), which will be approximated by the FLS in the observer design.

Assumption 1 [20]: The angle velocity ω is bounded.

B. INTEGRAL TERMINAL SLIDING MODE

A form of the integral terminal sliding mode is proposed in [38]:

$$s = x(t) - x(0) + \beta\int_0^t |x(\tau)|^\gamma \mathrm{sign}(x(\tau))d\tau, \quad (5)$$

where $x(t) \in R$ is the system state variable and $\beta > 0$ and $0 < \gamma < 1$ are design parameters.

It is obvious that $s(0) = 0$. This implies that the system starts on the integral terminal sliding mode surface (5) from the initial time instant.

Furthermore, on the sliding surface, $s = 0$, which results in

$$\dot{x}(t) + \beta|x(t)|^\gamma \mathrm{sign}(x(t)) = 0. \quad (6)$$

The finite time t_s that is taken from $x(0) \neq 0$ to $x(t_s) = 0$ is given by

$$t_s = \frac{1}{\beta(1-\gamma)}|x(0)|^{1-\gamma}. \quad (7)$$

C. FUZZY LOGIC SYSTEMS

The basic configuration of an FLS consists of four components: fuzzifier, fuzzy rule base, fuzzy inference engine, and defuzzifier. The fuzzy rule base is a collection of IF-THEN rules, and the lth fuzzy rule is written as

R^l: IF x_1 is F_1^l and ... and x_n is F_n^l, THEN z is G^l, where F_i^l and G^l are fuzzy sets associated with the fuzzy membership

functions $\mu_{F_i^l}(x_i)$ and $\mu_{G^l}(z)$, respectively, $i = 1, \cdots, n$, $l = 1, \cdots, L$, and L is the number of rules.

Based on these fuzzy IF-THEN rules, the FLS performs a mapping from an input vector $\chi = [x_1, \cdots, x_n]^T \in R^n$ to an output variable $z \in R$. If we use the strategy of singleton fuzzifier, product inference, and centre-average defuzzifier, the output of the FLS can be defined as follows:

$$z(\chi) = \frac{\sum_{l=1}^{L} z^l (\prod_{i=1}^{n} \mu_{F_i^l}(x_i))}{\sum_{l=1}^{L} \prod_{i=1}^{n} \mu_{F_i^l}(x_i)}, \tag{8}$$

where z^l is the point in G^l at which $\mu_{G^l}(z)$ obtains its maximum value 1.

For simplicity, $z(\chi)$ can be written in the following compact form:

$$z(\chi) = \hat{\theta}^T \xi(\chi) := \hat{f}(\chi|\hat{\theta}), \tag{9}$$

where $\hat{\theta} = [z^1, \cdots, z^L]^T$ is called the unknown parameter vector that is to be updated and $\xi(\chi) = [\xi^1(\chi), \cdots, \xi^L(\chi)]^T$ is called the fuzzy basis function vector, $\xi^l(\chi) = \frac{\prod_{i=1}^{n} \mu_{F_i^l}(x_i)}{\sum_{l=1}^{L} \prod_{i=1}^{n} \mu_{F_i^l}(x_i)}, l = 1, 2, \cdots, L$.

Lemma 1 [39]: Let $f(\chi)$ be a continuous function defined on a compact set Ω. Then, for any constant $\varepsilon > 0$, there exists a fuzzy system (9) such that $\sup_{\chi \in \Omega} |f(\chi) - \hat{f}(\chi|\hat{\theta})| \leq \varepsilon$.

III. OBSERVER DESIGN

Motivated by [40], the following adaptive fuzzy observer is proposed:

$$\begin{cases} \dot{\hat{x}} = \hat{v}\cos\phi - \hat{\omega} d \sin\phi + l_1 \tilde{x}\cos\phi - l_1 \tilde{y}\sin\phi, \\ \dot{\hat{y}} = \hat{v}\sin\phi + \hat{\omega} d \cos\phi + l_1 \tilde{x}\sin\phi + l_1 \tilde{y}\cos\phi, \\ \dot{\hat{\phi}} = \hat{\omega} + l_1 \tilde{\phi}, \\ \hat{v} = z_1 + l_2 \tilde{x}, \\ \hat{\omega} = z_2 + l_2 \tilde{\phi}, \\ \dot{z}_1 = \hat{g}_1(\hat{Y}_1|\hat{\theta}_1) + a_{11} U_1 + l_1 l_2 \tilde{x} + \varphi_1, \\ \dot{z}_2 = \hat{g}_2(\hat{Y}_2|\hat{\theta}_2) + a_{21} U_2 + l_1 l_2 \tilde{\phi} + \varphi_2, \end{cases} \tag{10}$$

where l_1 and l_2 are positive design parameters, $\tilde{x} = (x - \hat{x})\cos\phi + (y - \hat{y})\sin\phi$, $\tilde{y} = -(x - \hat{x})\sin\phi + (y - \hat{y})\cos\phi$, $\tilde{\phi} = \phi - \hat{\phi}$, $\hat{Y}_1 = [\hat{x}, \hat{y}, \hat{\phi}, \hat{v}, \hat{\omega}, \tilde{y}]^T$, $\hat{Y}_2 = [\hat{x}, \hat{y}, \hat{\phi}, \hat{v}, \hat{\omega}]^T$. φ_1 and φ_2 are designed, and $\hat{g}_1(\hat{Y}_1|\hat{\theta}_1)$ and $\hat{g}_2(\hat{Y}_2|\hat{\theta}_2)$ are illustrated below.

Based on (4) and (10), we can obtain the following observer error dynamics:

$$\begin{cases} \dot{\tilde{x}} = \tilde{v} - l_1 \tilde{x} + \tilde{y}\omega, \\ \dot{\tilde{y}} = \tilde{\omega} d - l_1 \tilde{y} - \tilde{x}\omega, \\ \dot{\tilde{\phi}} = \tilde{\omega} - l_1 \tilde{\phi}, \\ \dot{\tilde{v}} = g_1(Y_1) - \hat{g}_1(\hat{Y}_1|\hat{\theta}_1) - l_2 \tilde{v} - \varphi_1, \\ \dot{\tilde{\omega}} = g_2(Y_2) - \hat{g}_2(\hat{Y}_2|\hat{\theta}_2) - l_2 \tilde{\omega} - \varphi_2, \end{cases} \tag{11}$$

where $\tilde{v} = v - \hat{v}$, $\tilde{\omega} = \omega - \hat{\omega}$, $Y_1 = [x, y, \phi, v, \omega, \tilde{y}]^T$, $Y_2 = Y$, $g_1(Y_1) = f_1(Y) - a_{12} v - l_2 \tilde{y}\omega$, $g_2(Y_2) = f_2(Y) - a_{22}\omega$.

Using Lemma 1, for $i = 1, 2$, the unknown non-linear function $g_i(Y_i)$ can be approximated by the following FLS:

$$\hat{g}_i(Y_i|\hat{\theta}_i) = \hat{\theta}_i^T \xi_i(Y_i), \tag{12}$$

where $\xi_i(Y_i)$ is the fuzzy basis function vector and $\hat{\theta}_i$ is the parameter vector of each fuzzy system designed later.

For $i = 1, 2$, we define the optimal approximation parameters $\hat{\theta}_i^*$ as follows:

$$\hat{\theta}_i^* = \underset{\hat{\theta}_i \in \Omega_i}{\operatorname{argmin}} [\sup_{Y_i \in U} |g_i(Y_i) - \hat{g}_i(Y_i|\hat{\theta}_i)|],$$

where Ω_i is the compact set of allowable controller parameters. Moreover, the parameter error and the minimum approximation error are defined as $\tilde{\theta}_i = \hat{\theta}_i^* - \hat{\theta}_i$ and $\omega_i(Y_i) = g_i(Y_i) - \hat{g}_i(Y_i|\hat{\theta}_i^*)$, respectively.

IV. CONTROLLER DESIGN

It is assumed the reference trajectory $q_r(t) = [x_r(t), y_r(t), \phi_r(t)]^T$ is generated by a reference NWMR with the kinematic equation

$$\begin{cases} \dot{x}_r = v_r \cos\phi_r - \omega_r d \sin\phi_r, \\ \dot{y}_r = v_r \sin\phi_r + \omega_r d \cos\phi_r, \\ \dot{\phi}_r = \omega_r. \end{cases} \tag{13}$$

The objective of the trajectory tracking control is to design a strategy such that $q(t)$ converges asymptotically to $q_r(t)$, while all signals in the derived closed-loop system remain bounded. In this study, an auxiliary velocity controller v_c and ω_c are designed to allow the kinematic model to meet the control objective. Then, the actuator voltage control inputs u_1 and u_2 are designed for the dynamic model such that v and ω converge to ϑ_c and ω_c in finite time, respectively.

We define the tracking position errors as the difference between the centre of mass C of the NWMR and the centre of mass of the reference NWMR, as follows [1]:

$$\begin{cases} e_1 = (x_r - x)\cos\phi + (y_r - y)\sin\phi, \\ e_2 = -(x_r - x)\sin\phi + (y_r - y)\cos\phi, \\ e_3 = \phi_r - \phi. \end{cases} \tag{14}$$

The time derivatives of the tracking position errors are given as

$$\begin{cases} \dot{e}_1 = -(\tilde{v} + \hat{v}) + (\tilde{\omega} + \hat{\omega}) e_2 + v_r \cos e_3 - \omega_r d \sin e_3, \\ \dot{e}_2 = -(e_1 + d)(\tilde{\omega} + \hat{\omega}) + v_r \sin e_3 + \omega_r d \cos e_3, \\ \dot{e}_3 = \omega_r - (\tilde{\omega} + \hat{\omega}). \end{cases} \tag{15}$$

Therefore, the objective of this study becomes to design an auxiliary velocity controller that can make the tracking position errors all asymptotically converge to zero. In this study, the auxiliary velocity controllers v_c and ω_c are designed as follows, from [38] and [41]:

$$\begin{cases} v_c = v_r \cos e_3 + k_1 (e_1 + d - d\cos e_3), \\ \omega_c = \omega_r + k_3 v_r (e_2 - d \sin e_3) + k_2 \sin e_3, \end{cases} \tag{16}$$

where k_1, k_2, and k_3 are positive design parameters.

Substituting (16) into (15), the closed-loop kinematic equation can be written as

$$\begin{cases} \dot{e}_1 = -[\tilde{v} + v_r \cos e_3 + k_1(e_1 + d - d\cos e_3)] \\ \qquad + [\tilde{\omega} + \omega_r + k_3 v_r(e_2 - d \sin e_3) \\ \qquad + k_2 \sin e_3]e_2 + v_r \cos e_3 - \omega_r d \sin e_3, \\ \dot{e}_2 = -(e_1 + d)[\tilde{\omega} + \omega_r + k_3 v_r(e_2 - d \sin e_3) \\ \qquad + k_2 \sin e_3] + v_r \sin e_3 + \omega_r d \cos e_3, \\ \dot{e}_3 = \omega_r - [\tilde{\omega} + \omega_r + k_3 v_r(e_2 - d \sin e_3) \\ \qquad + k_2 \sin e_3]. \end{cases} \tag{17}$$

Now, we design φ_1 and φ_2 of the observer (10) as follows:

$$\begin{cases} \varphi_1 = \tilde{x} - (e_1 + d - d\cos e_3), \\ \varphi_2 = \tilde{y}d + \tilde{\phi} - \dfrac{\sin e_3}{k_3}. \end{cases} \tag{18}$$

Additionally, we use the following adaptation laws to adjust the unknown parameters θ_1 and θ_2:

$$\begin{cases} \dot{\hat{\theta}}_1 = \mu_1 \hat{v}[\xi_1(\hat{Y}_1) - \sigma_1 \operatorname{sign}(\hat{v})\hat{\theta}_1], \\ \dot{\hat{\theta}}_2 = \mu_2 \hat{\omega}[\xi_2(\hat{Y}_2) - \sigma_2 \operatorname{sign}(\hat{\omega})\hat{\theta}_2], \end{cases} \tag{19}$$

where μ_i and σ_i, $i = 1, 2$, are positive design parameters.

Remark 3: Compared to the adaptation laws in [40], the above adaptation laws do not contain differential and integral operations with respect to $\hat{\theta}_i$ and $\xi_i(Y_i)$, $i = 1, 2$. Therefore, the adaptation laws (19) can be realized more easily.

Similar to [42], we can prove the following Lemma:

Lemma 2: For $i = 1, 2, \hat{\theta}_i$ is bounded in (19) by $\|\hat{\theta}_i\| \le \frac{\sqrt{L}}{\sigma_i}$, where L is the number of rules.

Theorem 1: For model (4) of the NWMR, if the observer is designed as (10) with (18) and (19) and the auxiliary velocity controller is designed as (16), then the observer errors and tracking position errors will be uniformly ultimately bounded.

Proof: We consider the following Lyapunov function candidate:

$$V_1 = V_{11} + V_{12}, \tag{20}$$

where

$$V_{11} = \frac{1}{2}(\tilde{x}^2 + \tilde{y}^2 + \tilde{\phi}^2 + \tilde{v}^2 + \tilde{\omega}^2), \tag{21}$$

$$V_{12} = \frac{1}{2}(e_1 + d - d\cos e_3)^2 + \frac{1}{2}(e_2 - d \sin e_3)^2 + \frac{1 - \cos e_3}{k_3}. \tag{22}$$

Differentiating V_{11} with respect to time and substituting (11) into it, we have

$$\begin{aligned} \dot{V}_{11} = & -l_1\tilde{x}^2 - l_1\tilde{y}^2 - l_1\tilde{\phi}^2 - l_2\tilde{v}^2 - l_2\tilde{\omega}^2 \\ & + \tilde{v}[g_1(Y_1) - \hat{g}_1(\hat{Y}_1|\hat{\theta}_1)] + \tilde{\omega}[g_2(Y_2) - \hat{g}_2(\hat{Y}_2|\hat{\theta}_2)] \\ & + \tilde{x}\tilde{v} + \tilde{y}\tilde{\omega}d + \tilde{\phi}\tilde{\omega} - \tilde{v}\varphi_1 - \tilde{\omega}\varphi_2. \end{aligned} \tag{23}$$

Differentiating V_{12} with respect to time and substituting (17) into it, we have

$$\begin{aligned} \dot{V}_{12} = & -k_1(e_1 + d - d\cos e_3)^2 - \frac{k_2}{k_3}\sin^2 e_3 \\ & - \tilde{v}(e_1 + d - d\cos e_3) - \tilde{\omega}\frac{\sin e_3}{k_3}. \end{aligned} \tag{24}$$

Substituting (18), (23), and (24) into (20), one obtains

$$\begin{aligned} \dot{V}_1 = & -l_1\tilde{x}^2 - l_1\tilde{y}^2 - l_1\tilde{\phi}^2 - l_2\tilde{v}^2 - l_2\tilde{\omega}^2 \\ & - k_1(e_1 + d - d\cos e_3)^2 - \frac{k_2}{k_3}\sin^2 e_3 \\ & + \tilde{v}[g_1(Y_1) - \hat{g}_1(\hat{Y}_1|\hat{\theta}_1)] \\ & + \tilde{\omega}[g_2(Y_2) - \hat{g}_2(\hat{Y}_2|\hat{\theta}_2)]. \end{aligned} \tag{25}$$

For $i = 1, 2$, the following equality holds, from [43]:

$$\begin{aligned} & g_i(Y_i) - \hat{g}_i(\hat{Y}_i|\hat{\theta}_i) \\ & = g_i(Y_i) - \hat{g}_i(Y_i|\hat{\theta}_i^*) + \hat{g}_i(Y_i|\hat{\theta}_i^*) - \hat{g}_i(\hat{Y}_i|\hat{\theta}_i^*) \\ & \quad + \hat{g}_i(\hat{Y}_i|\hat{\theta}_i^*) - \hat{g}_i(\hat{Y}_i|\hat{\theta}_i) \\ & = \omega_i(Y_i) + \theta_i^{*T}[\xi_i(Y_i) - \xi_i(\hat{Y}_i)] + \tilde{\theta}_i^T \xi_i(\hat{Y}_i). \end{aligned} \tag{26}$$

From Lemma 1, Lemma 2, and the boundedness of $\xi_i(Y_i)$ and $\xi_i(\hat{Y}_i)$, it can be obtained that $g_i(Y_i) - \hat{g}_i(\hat{Y}_i|\hat{\theta}_i)$ is bounded. That is, there exist unknown constants d_{1i} such that $|g_i(Y_i) - \hat{g}_i(\hat{Y}_i|\hat{\theta}_i)| \le d_{1i}$, $i = 1, 2$. Moreover, we can get

$$\begin{aligned} \dot{V}_1 \le & -l_1\tilde{x}^2 - l_1\tilde{y}^2 - l_1\tilde{\phi}^2 - l_2\tilde{v}^2 - l_2\tilde{\omega}^2 \\ & - k_1(e_1 + d - d\cos e_3)^2 - \frac{k_2}{k_3}\sin^2 e_3 \\ & + |\tilde{v}|d_{11} + |\tilde{\omega}|d_{12}. \end{aligned} \tag{27}$$

Using Young's inequality yields

$$\begin{aligned} \dot{V}_1 \le & -l_1\tilde{x}^2 - l_1\tilde{y}^2 - l_1\tilde{\phi}^2 - (l_2 - \frac{1}{2})\tilde{v}^2 - (l_2 - \frac{1}{2})\tilde{\omega}^2 \\ & - k_1(e_1 + d - d\cos e_3)^2 - \frac{k_2}{k_3}\sin^2 e_3 \\ & + \frac{1}{2}d_{11}^2 + \frac{1}{2}d_{12}^2. \end{aligned} \tag{28}$$

Denote

$$\begin{aligned} \bar{V}_1 = & \, l_1\tilde{x}^2 + l_1\tilde{y}^2 + l_1\tilde{\phi}^2 + (l_2 - \frac{1}{2})\tilde{v}^2 + (l_2 - \frac{1}{2})\tilde{\omega}^2 \\ & + k_1(e_1 + d - d\cos e_3)^2 + \frac{k_2}{k_3}\sin^2 e_3. \end{aligned}$$

It is noted that $\bar{V}_1$ is positive definite, provided that we choose $l_2 > \frac{1}{2}$. If $\bar{V}_1 > \frac{1}{2}d_{11}^2 + \frac{1}{2}d_{12}^2$, it follows that $\dot{V}_1 < 0$. According to Lyapunov stability theory [44], $\tilde{x}, \tilde{y}, \tilde{\phi}, \tilde{v}, \tilde{\omega}, e_1, e_2$ and e_3 all converge asymptotically to zero. Thus, $\bar{V}_1$ converges to zero, which contradicts $\bar{V}_1 > \frac{1}{2}d_{11}^2 + \frac{1}{2}d_{12}^2$. Therefore, $\bar{V}_1$ is bounded by $\frac{1}{2}d_{11}^2 + \frac{1}{2}d_{12}^2$. That is, $\bar{V}_1 \le \frac{1}{2}d_{11}^2 + \frac{1}{2}d_{12}^2$. As a result, $\tilde{x}, \tilde{y}, \tilde{\phi}, \tilde{v}, \tilde{\omega}, e_1, e_2$, and e_3 are uniformly ultimately bounded.

Now, it remains to design the actuator voltage control inputs u_1 and u_2 so ϑ_c and ω_c can be obtained in finite time. In this study, the auxiliary velocity tracking errors are defined as $e_{\vartheta 1} = v_c - \hat{v}$ and $e_{\vartheta 2} = \omega_c - \hat{\omega}$.

A continuous non-singular integral terminal sliding mode is defined as in the form (5):

$$\begin{cases} s_1 = e_{\vartheta 1} - e_{\vartheta 1}(0) + \beta_1 \int_0^t |e_{\vartheta 1}|^{\gamma_1} \operatorname{sign}(e_{\vartheta 1}) d\tau, \\ s_2 = e_{\vartheta 2} - e_{\vartheta 2}(0) + \beta_2 \int_0^t |e_{\vartheta 2}|^{\gamma_2} \operatorname{sign}(e_{\vartheta 2}) d\tau, \end{cases} \tag{29}$$

where $\beta_i > 0$ and $0 < \gamma_i < 1, i = 1, 2$, are design parameters.

The time derivative of s_1 and s_2 yields

$$\begin{cases} \dot{s}_1 = \dot{v}_c - \hat{g}_1(\hat{Y}_1|\hat{\theta}_1) - a_{11}U_1 - l_2\tilde{v} - l_2\tilde{y}\omega \\ \qquad -\tilde{x} + e_1 + d - d\cos e_3 + \beta_1 |e_{\vartheta 1}|^{\gamma_1} \operatorname{sign}(e_{\vartheta 1}), \\ \dot{s}_2 = \dot{\omega}_c - \hat{g}_2(\hat{Y}_2|\hat{\theta}_2) - a_{21}U_2 - l_2\tilde{\omega} \\ \qquad -\tilde{y}d - \tilde{\phi} + \dfrac{\sin e_3}{k_3} + \beta_2 |e_{\vartheta 2}|^{\gamma_2} \operatorname{sign}(e_{\vartheta 2}). \end{cases} \tag{30}$$

By virtue of Assumption 1 and Theorem 1, $l_2\tilde{v} + l_2\tilde{y}\omega$ and $l_2\tilde{\omega}$ are bounded. It is assumed that there exist unknown positive constants d_{21} and d_{22} such that $|l_2\tilde{v} + l_2\tilde{y}\omega| \le d_{21}$ and $|l_2\tilde{\omega}| \le d_{22}$.

Let

$$\begin{cases} U_1 = \dfrac{1}{a_{11}}[\dot{v}_c - \hat{g}_1(\hat{Y}_1|\hat{\theta}_1) - \tilde{x} + e_1 + d - d\cos e_3 \\ \qquad +\beta_1 |e_{\vartheta 1}|^{\gamma_1} \operatorname{sign}(e_{\vartheta 1}) \\ \qquad +k_{11}s_1 + k_{12}|s_1|^{\rho} \operatorname{sign}(s_1) + u_{r1}], \\ U_2 = \dfrac{1}{a_{21}}[\dot{\omega}_c - \hat{g}_2(\hat{Y}_2|\hat{\theta}_2) \\ \qquad -\tilde{y}d - \tilde{\phi} + \dfrac{\sin e_3}{k_3} + \beta_2 |e_{\vartheta 2}|^{\gamma_2} \operatorname{sign}(e_{\vartheta 2}) \\ \qquad +k_{21}s_2 + k_{22}|s_2|^{\rho} \operatorname{sign}(s_2) + u_{r2}], \end{cases} \tag{31}$$

where $k_{ij} > 0, i = 1, 2, j = 1, 2$, and $0 < \rho < 1$ are design parameters, while u_{ri}, $i = 1, 2$, are robust controllers. For $i = 1, 2$, u_{ri} is designed as

$$u_{ri} = (\hat{d}_{2i} + \eta_i) \operatorname{sign}(s_i), \tag{32}$$

where $\hat{d}_{2i}$ is the estimate of d_{2i}, $\tilde{d}_{2i} = d_{2i} - \hat{d}_{2i}$ is the estimate error, and η_i is a positive design parameter.

We use the following adaptation laws to adjust the unknown constant $\hat{d}_{2i}$:

$$\dot{\hat{d}}_{2i} = \varsigma_i s_i \operatorname{sign}(s_i), \tag{33}$$

where ς_i, $i = 1, 2$, are positive design parameters.

Furthermore, the following actuator voltage control input is obtained:

$$\begin{cases} u_1 = \frac{1}{2}(U_1 + U_2), \\ u_2 = \frac{1}{2}(U_1 - U_2). \end{cases} \tag{34}$$

Substituting (31) into (30), we have the closed-loop dynamic equation:

$$\begin{cases} \dot{s}_1 = -k_{11}s_1 - k_{12}|s_1|^{\rho} \operatorname{sign}(s_1) - l_2\tilde{v} - l_2\tilde{y}\omega - u_{r1}, \\ \dot{s}_2 = -k_{21}s_2 - k_{22}|s_2|^{\rho} \operatorname{sign}(s_2) - l_2\tilde{\omega} - u_{r2}. \end{cases} \tag{35}$$

The properties of the proposed adaptive fuzzy output feedback control law are summarized by the following theorem:

Theorem 2: For model (4) of the NWMR, if the integral terminal sliding mode is chosen following (29) and the actuator voltage control input with the robust controller (32) and adaptation laws (33) is designed following (34), then

(1) all of the signals in the closed system are bounded;

(2) for $i = 1, 2$, the sliding variable s_i will converge to the region $|s_i| \le \delta_i$ in finite time, where

$$\delta_1 = \min\{\frac{|\tilde{d}_{21}|}{k_{11}}, (\frac{|\tilde{d}_{21}|}{k_{12}})^{\frac{1}{\rho}}\}, \quad \delta_2 = \min\{\frac{|\tilde{d}_{22}|}{k_{21}}, (\frac{|\tilde{d}_{22}|}{k_{22}})^{\frac{1}{\rho}}\}.$$

Moreover, the auxiliary velocity tracking error e_{vi} will converge to the region $e_{\vartheta i} \le 2\delta_i + |e_{\vartheta i}(0)|$ in finite time.

To prove Theorem 2, we introduce two lemmas.

Lemma 3 [32]: Suppose $a_1, a_2, \cdots, a_n$ are all positive numbers and $0 < p < 2$; then, the following inequality holds:

$$(a_1^2 + a_2^2 + \cdots + a_n^2)^p \le (a_1^p + a_2^p + \cdots + a_n^p)^2. \tag{36}$$

Lemma 4 [32]: An extended Lyapunov description of finite time stability can be given with the form of fast terminal sliding mode as

$$\dot{V}(x) + \alpha V(x) + \beta V^{\gamma}(x) \le 0, \quad \alpha, \beta > 0, \ 0 < \gamma < 1, \tag{37}$$

and the settling time can be given by

$$t_r \le \frac{1}{\alpha(1-\gamma)} \ln \frac{\alpha V^{1-\gamma}(x(0)) + \beta}{\beta}. \tag{38}$$

Proof of Theorem 2: We consider the following Lyapunov function candidate:

$$V_2 = V_{21} + V_{22}. \tag{39}$$

where

$$V_{21} = \frac{1}{2}(s_1^2 + s_2^2), \tag{40}$$

$$V_{22} = \frac{\tilde{d}_{21}^2}{2\varsigma_1} + \frac{\tilde{d}_{22}^2}{2\varsigma_2}. \tag{41}$$

(1) Differentiating V_{21} with respect to time and substituting (35) into it, we have

$$\begin{aligned} \dot{V}_{21} = & -k_{11}s_1^2 - k_{12}|s_1|^{\rho+1} - k_{21}s_2^2 - k_{22}|s_2|^{\rho+1} \\ & - s_1(l_2\tilde{v} + l_2\tilde{y}\omega) - s_2 l_2\tilde{\omega} - s_1 u_{r1} - s_2 u_{r2}. \end{aligned} \tag{42}$$

Substituting (32) into (42), the following inequality holds:

$$\begin{aligned} \dot{V}_{21} \le & -k_{11}s_1^2 - k_{12}|s_1|^{\rho+1} - k_{21}s_2^2 - k_{22}|s_2|^{\rho+1} \\ & + |s_1|d_{21} + |s_2|d_{22} - |s_1|(\hat{d}_{21} + \eta_1) - |s_2|(\hat{d}_{22} + \eta_2). \end{aligned} \tag{43}$$

Therefore

$$\begin{aligned} \dot{V}_{21} \le & -k_{11}s_1^2 - k_{12}|s_1|^{\rho+1} - k_{21}s_2^2 - k_{22}|s_2|^{\rho+1} \\ & + |s_1|\tilde{d}_{21} + |s_2|\tilde{d}_{22}. \end{aligned} \tag{44}$$

Differentiating V_{22} with respect to time and applying the adaptation laws (33) in it, we have

$$\dot{V}_{22} = -\frac{\tilde{d}_{21}\dot{\hat{d}}_{21}}{\varsigma_1} - \frac{\tilde{d}_{22}\dot{\hat{d}}_{22}}{\varsigma_2} = -|s_1|\tilde{d}_{21} - |s_2|\tilde{d}_{22}. \quad (45)$$

Combining (44) with (45) yields

$$\begin{aligned}\dot{V}_2 &= \dot{V}_{21} + \dot{V}_{22} \\ &\le -k_{11}s_1^2 - k_{12}|s_1|^{\rho+1} - k_{21}s_2^2 - k_{22}|s_2|^{\rho+1}. \end{aligned} \quad (46)$$

It is concluded that all of the signals s_i, e_{vi}, and d_{2i}, $i = 1, 2$, are bounded.

(2) We change (44) into the following four forms:

$$\begin{aligned}\dot{V}_{21} \le& -(k_{11} - \frac{\tilde{d}_{21}}{|s_1|})s_1^2 - (k_{21} - \frac{\tilde{d}_{22}}{|s_2|})s_2^2 \\ &- k_{12}|s_1|^{\rho+1} - k_{22}|s_2|^{\rho+1}, \end{aligned} \quad (47)$$

$$\begin{aligned}\dot{V}_{21} \le& -k_{11}s_1^2 - k_{21}s_2^2 - (k_{12} - \frac{\tilde{d}_{21}}{|s_1|^{\rho}})|s_1|^{\rho+1} \\ &- (k_{22} - \frac{\tilde{d}_{22}}{|s_2|^{\rho}})|s_2|^{\rho+1}, \end{aligned} \quad (48)$$

$$\begin{aligned}\dot{V}_{21} \le& -(k_{11} - \frac{\tilde{d}_{21}}{|s_1|})s_1^2 - k_{21}s_2^2 - k_{12}|s_1|^{\rho+1} \\ &- (k_{22} - \frac{\tilde{d}_{22}}{|s_2|^{\rho}})|s_2|^{\rho+1}, \end{aligned} \quad (49)$$

$$\begin{aligned}\dot{V}_{21} \le& -k_{11}s_1^2 - (k_{21} - \frac{\tilde{d}_{22}}{|s_2|})s_2^2 \\ &- (k_{12} - \frac{\tilde{d}_{21}}{|s_1|^{\rho}})|s_1|^{\rho+1} - k_{22}|s_2|^{\rho+1}. \end{aligned} \quad (50)$$

Case 1: If $k_{11} > \frac{|\tilde{d}_{21}|}{|s_1|}, k_{21} > \frac{|\tilde{d}_{22}|}{|s_2|}, k_{12} > \frac{|\tilde{d}_{21}|}{|s_1|^{\rho}}, k_{22} > \frac{|\tilde{d}_{22}|}{|s_2|^{\rho}}$, each form of (47), (48), (49), and (50) can be denoted as

$$\dot{V}_{21} \le -\bar{k}_{11}s_1^2 - \bar{k}_{21}s_2^2 - \bar{k}_{12}|s_1|^{\rho+1} - \bar{k}_{22}|s_2|^{\rho+1}, \quad (51)$$

where $\bar{k}_{11} = k_{11}$ or $k_{11} - \frac{\tilde{d}_{21}}{|s_1|}$, $\bar{k}_{21} = k_{21}$ or $k_{21} - \frac{\tilde{d}_{22}}{|s_2|}$, $\bar{k}_{12} = k_{12}$ or $k_{12} - \frac{\tilde{d}_{21}}{|s_1|^{\rho}}$, $\bar{k}_{22} = k_{22}$ or $k_{22} - \frac{\tilde{d}_{22}}{|s_2|^{\rho}}$, which are all positive design parameters.

By denoting $\lambda_1 = \min\{\bar{k}_{11}, \bar{k}_{21}\}, \lambda_2 = \min\{\bar{k}_{12}, \bar{k}_{22}\}$, we can get

$$\dot{V}_{21} \le -\lambda_1(s_1^2 + s_2^2) - \lambda_2(|s_1|^{\rho+1} + |s_2|^{\rho+1}). \quad (52)$$

Applying Lemma 3 to (52) yields

$$\dot{V}_{21} \le -\lambda_1(s_1^2 + s_2^2) - \lambda_2(s_1^2 + s_2^2)^{\frac{\rho+1}{2}}. \quad (53)$$

After some manipulations, we obtain

$$\dot{V}_{21} + 2\lambda_1 V_{21} + \lambda_2 2^{\frac{\rho+1}{2}} V_{21}^{\frac{\rho+1}{2}} \le 0. \quad (54)$$

From Lemma 4, it follows that s_1 and s_2 will all converge to zero in finite time,

$$t_r \le \frac{1}{\lambda_1(1-\rho)} \ln \frac{2\lambda_1 V_{21}^{(1-\rho)/2}(0) + \lambda_2 2^{(\rho+1)/2}}{\lambda_2 2^{(\rho+1)/2}}. \quad (55)$$

Moreover, on the sliding mode surface, according to (7),

$$t_{si} = \frac{1}{\beta_i(1-\gamma_i)}|e_{\vartheta i}(0)|^{1-\gamma_i}, \quad i = 1, 2. \quad (56)$$

Therefore, the auxiliary velocity tracking error e_{ϑ_i} will converge to zero in finite time $t_i = t_r + t_{si}, i = 1, 2$.

Case 2: If $k_{11} \le \frac{|\tilde{d}_{21}|}{|s_1|}$ or $k_{21} \le \frac{|\tilde{d}_{22}|}{|s_2|}$ or $k_{12} \le \frac{|\tilde{d}_{21}|}{|s_1|^{\rho}}$ or $k_{22} \le \frac{|\tilde{d}_{22}|}{|s_2|^{\rho}}$, it can be obtained that $|s_1| \le \frac{|\tilde{d}_{21}|}{k_{11}}$ or $|s_2| \le \frac{|\tilde{d}_{22}|}{k_{21}}$ or $|s_1| \le (\frac{|\tilde{d}_{21}|}{k_{12}})^{\frac{1}{\rho}}$ or $|s_2| \le (\frac{|\tilde{d}_{22}|}{k_{22}})^{\frac{1}{\rho}}$, respectively. Denote $\delta_1 = \min\{\frac{|\tilde{d}_{21}|}{k_{11}}, (\frac{|\tilde{d}_{21}|}{k_{12}})^{\frac{1}{\rho}}\}, \delta_2 = \min\{\frac{|\tilde{d}_{22}|}{k_{21}}, (\frac{|\tilde{d}_{22}|}{k_{22}})^{\frac{1}{\rho}}\}$. As a result, $|s_i| \le \delta_i, i = 1, 2$.

Combining Case 1 with Case 2, for $i = 1, 2$, we conclude that s_i will converge to the region $|s_i| \le \delta_i$ in finite time. Additionally, similarly to [38], it can be concluded that $e_{\vartheta i}$ will converge to region $e_{\vartheta i} \le 2\delta_i + |e_{\vartheta i}(0)|$ in finite time.

Remark 4: A drawback of the adaptive laws (33) is that they make the gain a monotonically increasing function which may create chattering or actuator saturation shown experimentally in [10]. In order to address this problem, the following robust controllers with an adaptive laws [11] are introduced:

$$u_{ri} = \begin{cases} (\hat{d}_{2i} + \eta_i)\text{sign}(s_i) & \text{if } |s_i| \ge \varepsilon_i, \\ (\hat{d}_{2i} + \eta_i)(\frac{s_i}{\varepsilon_i}) & \text{if } |s_i| < \varepsilon_i, \end{cases}$$

with

$$\dot{\hat{d}}_{2i} = \begin{cases} \varsigma_i|s_i|\text{sign}(s_i\dot{s}_i) & \text{if } \hat{d}_{2i} > \delta_i, \\ \varsigma_i\delta_i & \text{if } \hat{d}_{2i} \le \delta_i, \end{cases}$$

where $\varepsilon_i, \delta_i, i = 1, 2$, are also positive design parameters, and δ_i is utilized to keep $\hat{d}_{2i} > 0, i = 1, 2$. According to [11], all of the signals s_i, e_{vi}, and d_{2i}, $i = 1, 2$, are uniformly ultimate bounded. Moreover, the finite-time convergence of the sliding variables s_i and the auxiliary velocity tracking errors $e_{\vartheta i}, i = 1, 2$, can be proved similarly.

Remark 5: It is noted that the design parameters have some effects on the stability and performance of the closed-loop system. For example, the parameters l_i and $k_i, i = 1, 2$, have to be chosen sufficiently large to compensate the uncertainties of the system appearing in $\dot{V}_1$. Also, the parameters $k_{ij}, i = 1, 2, j = 1, 2$, have to be chosen sufficiently large to make the boundary $\delta_i, i = 1, 2$, small. However, increasing the above parameters will increase the level of control input and lead to actuators saturation and poor tracking performance. One may find them by gradually increasing them from small values and then by performing repeated simulations until acceptable robust and tracking performance are achieved. The similar method can be applied to adjust the parameters (such as k_3 and $\alpha_i, i = 1, 2$) which have to be chosen sufficiently smaller for good tracking performance. One needs to maintain a trade-off in the selection of controller parameters.

Remark 6: To avoid calculating $\dot{v}_c$ and $\dot{\omega}_c$, we can pass v_c and ω_c through the first-order filter:

$$\begin{cases} \alpha_1\dot{v}_f + v_f = v_c, \\ \alpha_2\dot{\omega}_f + \omega_f = \omega_c, \end{cases} \quad (57)$$

where $\alpha_i, i = 1, 2$, are positive filter time constants and $v_f(0) = v_c(0), \omega_f(0) = \omega_c(0)$. Moreover, by adjusting filter parameters, we can make the filter error as small as possible.

Remark 7: This paper has been focused on the design of a simple output feedback control system by using the FLS, velocity observer and integral terminal sliding mode. The parameter uncertainties (including mass and moment of inertia) and non-parameter uncertainties (including friction and external disturbances) are completely considered. However, the kinematic and dynamic perturbation due to wheel skidding and slipping are not taken into account in the design of the controller.

V. SIMULATION RESULTS

In this section, simulation results are provided to show the effectiveness of the proposed control strategy.

The parameters of the NWMR and its actuators are chosen to be equal to those in [20]: $m = 32\ kg, I = 19.455\ kgm^2, R = 0.75\ m, r = 0.15\ m, d = 0.3\ m, N = 20, K_b = 0.019, K_T = 0.2639\ Nm/A$, and $R_a = 1.6\Omega$. The lumped uncertainties are [16] and generated by $f = [0.8v + 0.5sign(v) + 3\sin(0.01t), 0.8\omega + 0.5sign(\omega) + 3\sin(0.01t)]^T$. In this simulation, the initial posture and velocity of the practical NWMR are taken as $q(0) = [0.1, 0.2, 0]^T$ and $\vartheta = [v, \omega]^T = [0, 0]^T$, respectively. The initial conditions of the observer are taken as $[\hat{x}, \hat{y}, \hat{\phi}, \hat{v}, \hat{\omega}]^T = [0, 0, 0, 0, 0]^T$.

The reference linear velocity and angular velocity are defined as $v_r(t) = 0.5$ and $\omega_r(t) = 1$, respectively. The trajectory of the reference NWMR is defined by (13). The initial posture of the reference NWMR is taken to be $q_r(0) = [0, 0, 0]^T$.

The objective of the trajectory tracking control is to design a strategy such that $q(t)$ converges asymptotically to $q_r(t)$, while all signals in the derived closed-loop system remain bounded. In the proposed control strategy, by utilizing the introduced adaptive fuzzy observer, an auxiliary velocity controller ϑ_c is designed to allow the kinematic model to meet the control objective. Then, the actuator voltage control input u is designed for the dynamic model such that ϑ converges to ϑ_c in finite time.

In the proposed adaptive fuzzy observer, the non-linear functions $g_1(Y_1) = f_1(Y) - a_{12}v - l_2\tilde{y}\omega$ and $g_2(Y_2) = f_2(Y) - a_{22}\omega$ are contained, where $Y_1 = [x, y, \phi, v, \omega, \tilde{y}]^T, Y_2 = [x, y, \phi, v, \omega]^T$. $g_1(Y_1)$ and $g_2(Y_2)$ are assumed to be completely unknown. The adaptive FLS $\hat{g}_1(Y_1|\hat{\theta}_1)$ and $\hat{g}_2(Y_2|\hat{\theta}_2)$ are used to approximate the unknown function $g_1(Y_1)$ and $g_2(Y_2)$, respectively. Since the velocities v and ω are unmeasured, the fuzzy systems have $x_1 = \hat{x}, x_2 = \hat{y}, x_3 = \hat{\phi}, x_4 = \hat{v}, x_5 = \hat{\omega}$ and $x_6 = \tilde{y}$ as inputs; thus, the fuzzy membership functions for each variable $x_i, i = 1, 2, \cdots, 6$ are chosen as

$$\mu_{F_i^1}(x_i) = \exp[-\frac{1}{2}(\frac{x_i + 1.25}{0.6})^2],$$
$$\mu_{F_i^2}(x_i) = \exp[-\frac{1}{2}(\frac{x_i}{0.6})^2],$$
$$\mu_{F_i^3}(x_i) = \exp[-\frac{1}{2}(\frac{x_i - 1.25}{0.6})^2].$$

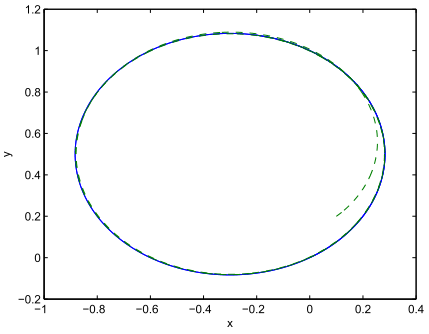

FIGURE 2. Reference trajectory (-) and actual trajectory (- -).

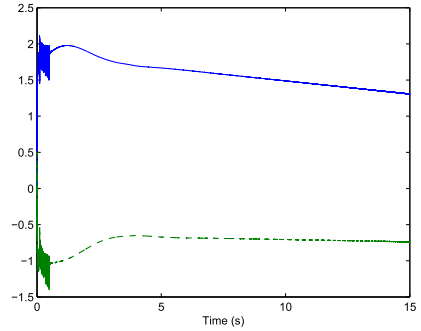

FIGURE 3. Actuator voltage input u_1 (-) and u_2 (- -).

The initial values of the estimated parameters $\hat{\theta}_{fi}(0)$ and $\hat{d}_{2i}(0), i = 1, 2$ are all set to 0.01.

The parameters of the observer and the control law are chosen to be $l_1 = 30, l_2 = 50, \mu_1 = \mu_2 = 0.5, \sigma_1 = \sigma_2 = 0.1$; $k_1 = 1, k_2 = 3, k_3 = 10$, and $\alpha_1 = \alpha_2 = 0.01$; and $\beta_1 = \beta_2 = 1, \gamma_1 = \gamma_2 = 0.8, k_{11} = k_{12} = k_{21} = k_{22} = 5, \rho = 0.3, \eta_1 = \eta_2 = 0.1$, and $\varsigma_1 = \varsigma_2 = 0.001$.

Using the proposed control strategy to control the NWMR, the simulation results are shown in Figs. 2-7. The trajectory tracking process in the X-Y plane of the NWMR is depicted in Fig. 2. Fig. 3 is the actuator voltage control input, which is bounded. The linear velocity v and the angle velocity ω, together with their observer values, are depicted in Fig. 4 and Fig. 5. It can be shown that the designed observer for the unmeasured velocities is valid. From Fig. 6, it can be observed that the auxiliary velocity tracking errors $e_{\vartheta 1}$ and $e_{\vartheta 2}$ converge to $|e_{\vartheta i}| \leq 5.909 \times 10^{-4}, i = 1, 2$, in finite time $t = 4.96\ s$. The tracking position errors e_1, e_2, and e_3 converge to $|e_i| \leq 2.402 \times 10^{-2}, i = 1, 2, 3$ in finite time $t = 3.124\ s$, which can be seen in Fig. 7.

To demonstrate the effectiveness of the proposed control strategy, by adopting the presented models and desired trajectory, another two simulations are performed.

Firstly, we use the conventional integral sliding mode [45] instead of the proposed integral terminal sliding mode in our control strategy, and the parameters and initial conditions are the same as those used in the initial simulation. The results of this simulation are illustrated in Figs. 8-10. It can be seen in Fig. 9 that the auxiliary velocity tracking errors $e_{\vartheta 1}$ and

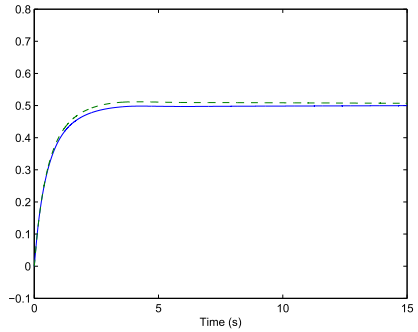

FIGURE 4. Linear velocity v (-) and observer linear velocity $\hat{v}$ (- -).

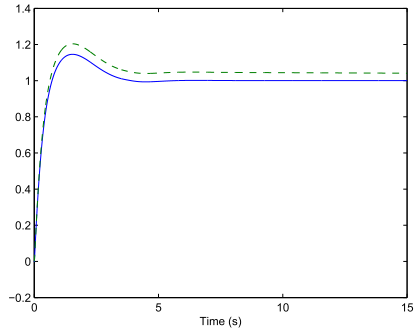

FIGURE 5. Angle velocity ω (-) and observer angle velocity $\hat{\omega}$ (- -).

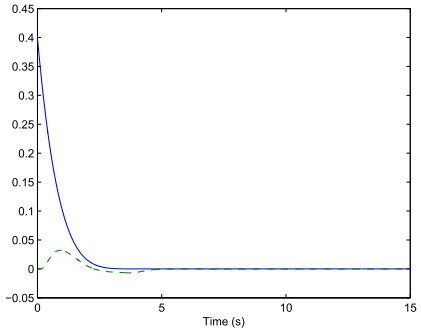

FIGURE 6. Auxiliary velocity tracking error $e_{\vartheta 1}$ (-) and $e_{\vartheta 2}$ (- -).

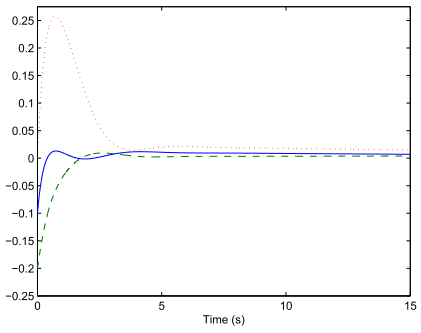

FIGURE 7. Tracking position error e_1 (-), e_2 (- -), and e_3 (. . .).

$e_{\vartheta 2}$ converge to $|e_{\vartheta i}| \leq 1.889 \times 10^{-3}$, $i = 1, 2$, in finite time $t = 8.105$ s. Fig. 10 shows that the tracking position errors e_1, e_2, and e_3 converge to $|e_i| \leq 2.42 \times 10^{-2}$, $i = 1, 2, 3$ in finite time $t = 5.654$ s.

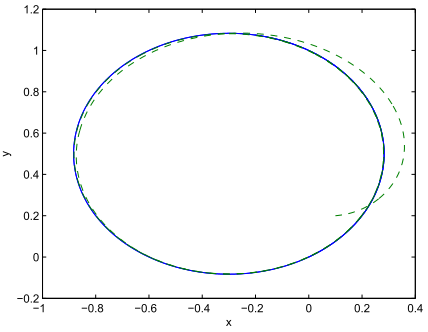

FIGURE 8. Reference trajectory (-) and actual trajectory (- -).

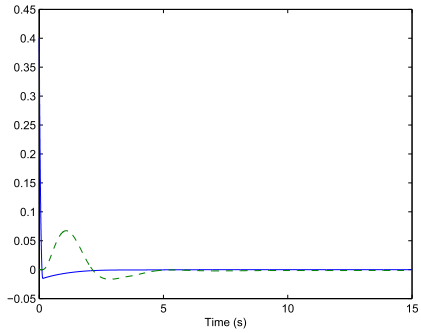

FIGURE 9. Auxiliary velocity tracking error $e_{\vartheta 1}$ (-) and $e_{\vartheta 2}$ (- -).

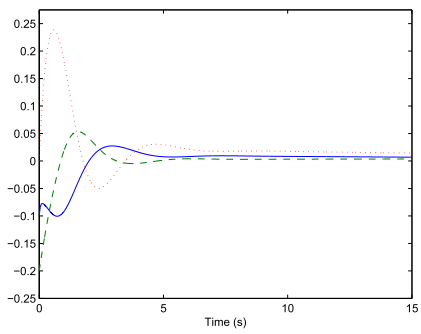

FIGURE 10. Tracking position error e_1 (-), e_2 (- -), and e_3 (. . .).

Secondly, we use the high-gain observer and control method in [27] instead of the proposed adaptive fuzzy observer and integral terminal sliding mode controller in our control strategy, respectively. Different from [27], an unknown function is approximated by the fuzzy logic system instead of the neural network. The parameters and initial conditions are also the same as those used in the initial simulation. The results of this simulation are plotted in Figs. 11-13. As shown by Fig. 12, the auxiliary velocity tracking errors $e_{\vartheta 1}$ and $e_{\vartheta 2}$ converge to $|e_{\vartheta i}| \leq 0.4221$, $i = 1, 2$, in finite time $t = 3.509$ s. Fig. 13 demonstrates that the tracking position errors e_1, e_2, and e_3 converge to $|e_i| \leq 0.1722$, $i = 1, 2, 3$, in finite time $t = 5.409$ s.

Based on the results of these simulations, it is concluded that the tracking position errors e_1, e_2, and e_3 all asymptotically converge to zero with faster responses when using the

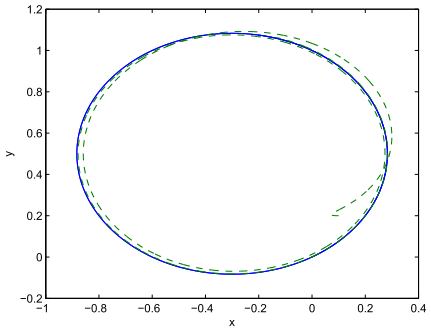

FIGURE 11. Reference trajectory (-) and actual trajectory (- -).

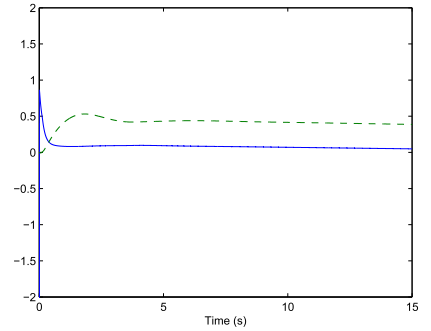

FIGURE 12. Auxiliary velocity tracking error $e_{\vartheta 1}$ (-) and $e_{\vartheta 2}$ (- -).

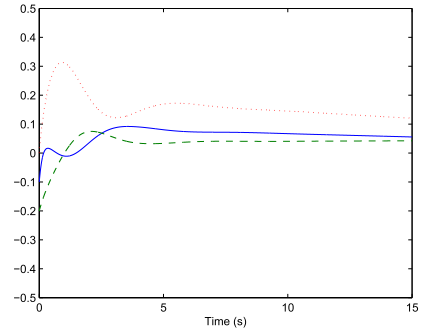

FIGURE 13. Tracking position error e_1 (-), e_2 (- -), and e_3 (. . .).

proposed control strategy. Therefore, by using the proposed control strategy, the practical NWMR can track the reference NWMR with better posture tracking performance, as seen in Fig. 2, Fig. 8, and Fig.10. These results are also obtained for the NWMR with parameter uncertainties, external disturbances, and without measuring velocity.

VI. CONCLUSION

In this paper, an adaptive fuzzy output feedback controller is given for the trajectory tracking problem of the NWMR with parameter uncertainties, external disturbances, and non-measurement of velocity. To address the total uncertainties and unmeasured velocities, an adaptive fuzzy observer is presented. Choosing the actuator voltage as the control input, a control strategy is proposed that includes an auxiliary velocity controller and an integral terminal sliding mode controller. It is shown that the auxiliary velocity tracking errors converge to a neighborhood near the origin in finite time, In addition, all the signals in the closed system are bounded. This leads to the tracking position errors converging asymptotically to a small neighborhood near the origin with a faster response than achieved by the existing controllers. The simulation results prove the feasibility of the proposed control strategy. However, wheel skidding and slipping are unavoidable due to tire deformation and other factors in real environments [46]. It is noted that time-delayed control is an alternate robust control method which does not depend on any uncertainty bounds. In the future, we will integrate time-delayed control with the integral terminal sliding control for the WMR with wheel skidding and slipping.

REFERENCES

[1] Y. Kanayama, Y. Kimura, F. Miyazaki, and T. Noguchi, "A stable tracking control method for an autonomous mobile robot," in *Proc. IEEE Int. Conf. Robot. Automat.*, vol. 1, May 1990, pp. 384–389.

[2] R. Fierro and F. L. Lewis, "Control of a nonholonomic mobile robot: Backstepping kinematics into dynamics," in *Proc. 34th Conf. Decis. Control*, Dec. 1995, pp. 3805–3810.

[3] P. Shu, M. Oya, and J. Zhao, "A new adaptive tracking control scheme of wheeled mobile robot without longitudinal velocity measurement," *Int. J. Robust Nonlinear Control*, vol. 28, no. 5, pp. 1789–1807, 2017. [Online]. Available: https://doi.org/10.1002/rnc.3985

[4] J. Huang, C. Wen, W. Wang, and Z.-P. Jiang, "Adaptive stabilization and tracking control of a nonholonomic mobile robot with input saturation and disturbance," *Syst. Control Lett.*, vol. 62, no. 3, pp. 234–241, Mar. 2013.

[5] L. Xin, Q. Wang, J. She, and Y. Li, "Robust adaptive tracking control of wheeled mobile robot," *Robot. Auton. Syst.*, vol. 78, pp. 36–48, Apr. 2016.

[6] S. Roy, S. B. Roy, and I. N. Kar, "Adaptive-robust control of Euler–Lagrange systems with linearly parametrizable uncertainty bound," *IEEE Trans. Control Syst. Technol.*, to be published, doi: 10.1109/TCST.2017.2739017.

[7] M. Begnini, D. W. Bertol, and N. A. Martins, "A robust adaptive fuzzy variable structure tracking control for the wheeled mobile robot: Simulation and experimental results," *Control Eng. Pract.*, vol. 64, pp. 27–43, Jul. 2017.

[8] M. Yue, L. Wang, and T. Ma, "Neural network based terminal sliding mode control for WMRs affected by an augmented ground friction with slippage effect," *IEEE/CAA J. Autom. Sinica*, vol. 4, no. 3, pp. 498–506, Jul. 2017.

[9] J. K. Lee, Y. H. Choi, and J. B. Park, "Sliding mode tracking control of mobile robots with approach angle in Cartesian coordinates," *Int. J. Control, Automat. Syst.*, vol. 13, no. 3, pp. 718–724, 2015.

[10] S. Roy, S. Nandy, R. Ray, and S. N. Shome, "Robust path tracking control of nonholonomic wheeled mobile robot: Experimental validation," *Int. J. Control Autom. Syst.*, vol. 13, no. 4, pp. 897–905, 2015.

[11] S. Roy and I. N. Kar, "Adaptive-robust control of uncertain Euler–Lagrange systems with past data: A time-delayed approach," in *Proc. IEEE Int. Conf. Robot. Automat. (ICRA)*, Stockholm, Sweden, May 2016, pp. 5715–5720.

[12] S. Roy, S. Nandy, I. N. Kar, R. Ray, and S. N. Shome, "Robust control of nonholonomic wheeled mobile robot with past information: Theory and experiment," *Proc. Inst. Mech. Eng. I, J. Syst. Control Eng.*, vol. 231, no. 3, pp. 178–188, 2017.

[13] S. Roy and I. N. Kar, "Adaptive sliding mode control of a class of nonlinear systems with artificial delay," *J. Franklin Inst.*, vol. 354, no. 18, pp. 8156–8179, 2017.

[14] Z.-G. Hou, A.-M. Zou, L. Cheng, and M. Tan, "Adaptive control of an electrically driven nonholonomic mobile robot via backstepping and fuzzy approach," *IEEE Trans. Control Syst. Technol.*, vol. 17, no. 4, pp. 803–815, Jul. 2009.

[15] B. S. Park, S. J. Yoo, J. B. Park, and Y. H. Choi, "A simple adaptive control approach for trajectory tracking of electrically driven nonholonomic mobile robots," *IEEE Trans. Control Syst. Technol.*, vol. 18, no. 5, pp. 1199–1206, Sep. 2010.

[16] K. Shojaei, A. M. Shahri, and A. Tarakameh, "Adaptive feedback linearizing control of nonholonomic wheeled mobile robots in presence of parametric and nonparametric uncertainties," *Robot. Comput.-Integr. Manuf.*, vol. 27, no. 1, pp. 194–204, 2011.

[17] T. Das and I. N. Kar, "Design and implementation of an adaptive fuzzy logic-based controller for wheeled mobile robots," *IEEE Trans. Control Syst. Technol.*, vol. 14, no. 3, pp. 501–510, May 2006.
[18] S. Roy, I. N. Kar, and J. Lee, "Toward position-only time-delayed control for uncertain Euler–Lagrange systems: Experiments on wheeled mobile robots," *IEEE Robot. Autom. Mag.*, vol. 2, no. 4, pp. 1925–1932, Oct. 2017.
[19] H. Nijmeijer and T. I. Fossen, Eds., *New Directions in Nonlinear Observer Design*. London, U.K.: Springer-Verlag, 1999.
[20] B. S. Park, S. J. Yoo, J. B. Park, and Y. H. Choi, "Adaptive output-feedback control for trajectory tracking of electrically driven non-holonomic mobile robots," *IET Control Theory Appl.*, vol. 5, no. 6, pp. 830–838, Apr. 2011.
[21] B. S. Park, J. B. Park, and Y. H. Choi, "Adaptive observer-based trajectory tracking control of nonholonomic mobile robots," *Int. J. Control, Automat., Syst.*, vol. 9, no. 3, pp. 534–541, 2011.
[22] K. D. Do, "Global output-feedback path-following control of unicycle-type mobile robots: A level curve approach," *Robot. Auton. Syst.*, vol. 74, pp. 229–242, Dec. 2015.
[23] K. Shojaei and A. M. Shahri, "Output feedback tracking control of uncertain non-holonomic wheeled mobile robots: A dynamic surface control approach," *IET Control Theory Appl.*, vol. 6, no. 2, pp. 216–228, 2012.
[24] M. A. Arteaga and R. Kelly, "Robot control without velocity measurements: New theory and experimental results," *IEEE Trans. Robot. Autom.*, vol. 20, no. 2, pp. 297–308, Apr. 2004.
[25] K. Shojaei, "Saturated output feedback control of uncertain nonholonomic wheeled mobile robots," *Robotica*, vol. 33, no. 1, pp. 87–105, 2015.
[26] J. Huang, C. Wen, W. wang, and Z.-P. Jiang, "Adaptive output feedback tracking control of a nonholonomic mobile robot," *Automatica*, vol. 50, no. 3, pp. 821–831, 2014.
[27] W. Zeng, Q. Wang, F. Liu, and Y. Wang, "Learning from adaptive neural network output feedback control of a unicycle-type mobile robot," *ISA Trans.*, vol. 61, pp. 337–347, Mar. 2016.
[28] W. Wang, C. Wen, J. Huang, and Z. Li, "Hierarchical decomposition based consensus tracking for uncertain interconnected systems via distributed adaptive output feedback control," *IEEE Trans. Autom. Control*, vol. 61, no. 7, pp. 1938–1945, Jul. 2016.
[29] W. Si, C. Wang, X. Dong, and W. Zeng, "Neural output-feedback control for time-delay systems with full-state constraints," *Control Decis.*, vol. 32, no. 9, pp. 1537–1546, 2017.
[30] M. Zhihong, A. P. Paplinski, and H. R. Wu, "A robust MIMO terminal sliding mode control scheme for rigid robotic manipulators," *IEEE Trans. Autom. Control*, vol. 39, no. 12, pp. 2464–2469, Dec. 1994.
[31] K.-B. Park and J.-J. Lee, "Comments on 'A robust MIMO terminal sliding mode control scheme for rigid robotic manipulators,'" *IEEE Trans. Autom. Control*, vol. 41, no. 5, pp. 761–762, May 1996.
[32] S. Yu, X. Yu, B. Shirinzadeh, and Z. Man, "Continuous finite-time control for robotic manipulators with terminal sliding mode," *Automatica*, vol. 41, no. 11, pp. 1957–1964, Nov. 2005.
[33] L. Wang, T. Chai, and L. Zhai, "Neural-network-based terminal sliding-mode control of robotic manipulators including actuator dynamics," *IEEE Trans. Ind. Electron.*, vol. 56, no. 9, pp. 3296–3304, Sep. 2009.
[34] T. Madani, B. Daachi, and K. Djouani, "Non-singular terminal sliding mode controller: Application to an actuated exoskeleton," *Mechatronics*, vol. 33, pp. 136–145, Feb. 2016.
[35] V. Nekoukar and A. Erfanian, "Adaptive fuzzy terminal sliding mode control for a class of MIMO uncertain nonlinear systems," *Fuzzy Sets Syst.*, vol. 179, no. 1, pp. 34–49, 2011.
[36] C.-S. Chiu, "Derivative and integral terminal sliding mode control for a class of MIMO nonlinear systems," *Automatica*, vol. 48, no. 2, pp. 316–326, 2012.
[37] D. Wang and C. B. Low, "Modeling and analysis of skidding and slipping in wheeled mobile robots: Control design perspective," *IEEE Trans. Robot.*, vol. 24, no. 3, pp. 676–687, Jun. 2008.
[38] S. Peng and W. Shi, "Adaptive fuzzy integral terminal sliding mode control of a nonholonomic wheeled mobile robot," *Math. Problems Eng.*, vol. 2017, no. 4, pp. 1–12, 2017, doi: 10.1155/2017/3671846.
[39] W. Shi, "Adaptive fuzzy control for multi-input multi-output nonlinear systems with unknown dead-zone inputs," *Appl. Soft Comput.*, vol. 30, pp. 36–47, May 2015.
[40] B. S. Park, J.-W. Kwon, and H. Kim, "Neural network-based output feedback control for reference tracking of underactuated surface vessels," *Automatica*, vol. 77, pp. 353–359, Mar. 2017.
[41] D. Huang, J. Zhai, W. Ai, and S. Fei, "Disturbance observer-based robust control for trajectory tracking of wheeled mobile robots," *Neurocomputing*, vol. 198, pp. 74–79, Jul. 2016.
[42] J. Na, X. Ren, and D. Zheng, "Adaptive control for nonlinear pure-feedback systems with high-order sliding mode observer," *IEEE Trans. Neural Netw. Learn. Syst.*, vol. 24, no. 3, pp. 370–382, Mar. 2013.
[43] W. Shi, "Observer-based indirect adaptive fuzzy control for SISO nonlinear systems with unknown gain sign," *Neurocomputing*, no. 171, pp. 1598–1605, Jan. 2016.
[44] J.-J. Slotine and W. Li, *Applied Nonlinear Control*. Englewood Cliffs, NJ, USA: Prentice-Hall, 1991.
[45] M. Yue, S. Wang, and Y. Zhang, "Adaptive fuzzy logic-based sliding mode control for a nonholonomic mobile robot in the presence of dynamic uncertainties," *Proc. Inst. Mech. Eng., C, J. Mech. Eng. Sci.*, vol. 229, no. 11, pp. 1979–1988, 2015.
[46] M. Chen, "Disturbance attenuation tracking control for wheeled mobile robots with skidding and slipping," *IEEE Trans. Ind. Electron.*, vol. 64, no. 4, pp. 3359–3368, Apr. 2017.

SHUYING PENG received the B.S. degree in mathematics from Qufu Normal University, Qufu, China, in 2002, and the M.S. degree in mathematics from Northwestern Polytechnical University, Xi'an, China, in 2005.

She is currently pursuing the Ph.D. degree with the School of Mechanical Engineering, Tianjin Polytechnic University, Tianjin, China. Her current research interests include fuzzy control theory and mobile robot control.

WUXI SHI received the B.S. degree in mathematics from Beijing Normal University, Beijing, China, in 1989, and the M.S. and Ph.D. degrees in control theory and control engineering from the Beijing University of Aeronautics and Astronautics, Beijing, China, in 1999 and 2003, respectively.

He is currently a Professor with the School of Electrical Engineering and Automation, Tianjin Polytechnic University, Tianjin, China. His current research interests include fuzzy control theory and fuzzy predictive control.